Supplementary Material:

Kinetics and thermodynamics of tetramolecular quadruplexes.

Jean-Louis Mergny, Anne de Cian, Amar Ghelab, Barbara Saccà & Laurent Lacroix

Laboratoire de Biophysique, Muséum National d'Histoire Naturelle USM503, INSERM U 565, CNRS UMR 5153, 43 rue Cuvier, 75231 Paris cedex 05 (France).

SUPPLEMENTARY FIGURES:

Figure S1: Isothermal difference spectra for some quadruplexes.

A *thermal difference spectrum* (TDS) is obtained for a nucleic acid by simply recording the ultraviolet absorbance spectra of the unfolded and folded states at temperatures above and below its melting temperature (T_m). The difference between these two spectra is the TDS. The TDS has a specific shape that is unique for quadruplexes (1)(Mergny *et al.,* in preparation), thus providing a simple, inexpensive and rapid method to gain structural insight into nucleic acid structures which is applicable to DNA and RNA from short oligomers to polynucleotides. The unusual thermal inertia of parallel quadruplexes also allowed us to record *isothermal difference spectra*. By convention, we chose to subtract the absorbance of the folded form from the spectrum of the unstructured oligonucleotide. These isothermal difference spectra are similar, but not identical, to TDS, as the absorbance spectra of the pure species (single-strands or quadruplexes) are temperature-dependent. Spectra were recorded between 220 and 335 nm with a Kontron Uvikon 940 UV/Vis spectrophotometer using quartz cuvettes with an optical pathlength of 0.2 or 1 cm. The spectra confirmed that the oligonucleotides adopted a quadruplex conformation.

a) Isothermal difference spectra at 20°C in NaCl for 5 different sequences at 15 or 30 µM strand concentration: filled circles: d-$(TG_5)_4$; vertical crosses, full line: d-$(TG_4)_4$; squares: d-$(T_2G_5)_4$; circles: d-$(TG_5T)_4$; crosses: d-$(TG_6T)_4$;

b) Isothermal difference spectra at 20°C in NaCl for 7 different sequences (100 µM): filled circles: d-$(TG_4)_4$; vertical crosses, full line: d-$(TG_4T)_4$; squares: d-$(G_4T)_4$; circles: d-$(G_4T_2)_4$; crosses: d-$(T_2G_4)_4$; circles/crosses: d-$(AG_4)_4$; little crosses: d-$(AG_4T)_4$

Note that the differential absorbance spectra are relatively similar, except for d-$(G_4T)_4$ and d-$(G_4T_2)_4$ which also exhibit unusual migration on a non-denaturing gel (figure S4).

Figure S2: Fitting procedure.

a) Example of excellent agreement between experimental data at two wavelengths (240 and 295 nm, blue and red, respectively) and equation (2). d-TG_6T oligonucleotide at 15 µM strand concentration in a 0.11M Na^+ pH 7.2 buffer at 12°C. Inserts: results fitted by Kaleidagraph 3.5 software. m0 = time; m2 is the association rate constant; m3 the final absorbance, m4 the initial absorbance (at t=m0=0, no quadruplex formed). The fitting formula in Kaleidagraph format is therefore
M3+((M4-M3)*((1+((4-1)*M2*(0.000015^(4-1)))*M0))^(1/(1-4))).
(0.000015 corresponds to the strand concentration, in M)

b) Example of poor matching between the fits at two different wavelengths (240 and 295 nm, blue and red, respectively). Different kinetic parameters (k_{on} values –"m2"- 2.8 10^9 and 1.7 10^{10} $M^{-3}.s^{-1}$) are deduced from the curves recorded at 240 and 295 nm (conflicting results are also found at different concentrations). d-AG_4 oligonucleotide at 30 µM strand concentration in a 0.11M K^+ pH 7.2 buffer at 11°C.

It is sometimes possible to resolve conflicting values by using lower strand concentrations (but not in this case). In our experience, k_{on} values found at sub-optimal strand concentration

are more reliable than those found at supra-optimal concentration. In the latter case, significant quadruplex formation is already obtained after a few minutes, and it is therefore difficult to extrapolate the absorbance A_0 to t=0 (no quadruplex). Errors in A_0 determination result in large errors in k_{on}.

c) Example of experimental data that cannot be fitted. d-G_4T oligonucleotide at 100 µM strand concentration in a 0.11 M Na^+ pH 7.2 buffer at 3°C. The association process is obviously more complicated than the usual model. (Also note that, as in case B, strand concentration was too high).

Figure S3: Dual wavelength parametric test of the two state model (2).

a) Example of excellent linear fit between A_{240nm} an A_{295nm}.

b) Example of poor adequation.

Experimental data taken from the experiment presented in figures S2A and S2B, respectively.

Figure S4: Non-denaturing gel electrophoresis of parallel quadruplexes

Formation of G4 DNA was evidenced by PAGE as previously described. Briefly, non-radiolabeled oligodeoxynucleotides (200 µM strand concentration) were preincubated 1 day at 4°C in a 0.11 M KCl (or NaCl, data not shown) 10 mM lithium cacodylate pH 7.2 buffer, then loaded on a 20% polyacrylamide gel containing 1X TBE and 20 mM KCl (Migration temperature 20°C). Quadruplexes were revealed by an anomalously slow migrating band, which was revealed by UV-shadowing with a UV light source (254 nm) and a digital camera. Radioactive labeling (with ^{32}P and T4-kinase) was not chosen, as the presence of a terminal 5' phosphate may interfere with the formation of some higher order quadruplex structures (quadruplex dimers) (3). T_6-T_{18}: single-stranded markers corresponding to dT_{6-18}

oligodeoxynucleotides. In each pair of lanes, the oligonucleotide is loaded "single-stranded" (incubation by omitting KCl, and boiling prior to loading) or after a 3-day long incubation at 4°C in 0.01 M KCl. In most cases, a single quadruplex band is found. Note that d-$(TG_6T)_4$ quadruplex was not disrupted by boiling, whereas quadruplex formation for d-TG_3T and d-T_2AG_3 was only partial after 1 day at this ionic strength. The d-$(AG_4)_4$ and d-$(AG_4T)_4$ "quadruplexes", also slower than single-strands, are still unusually fast compared to other quadruplexes.

Figure S5: Effect of pH.

a) Effect of pH on k_{on} followed at 295 nm. d-TG_4T oligonucleotide (determined at 3°C 0.1 mM strand concentration) in a 0.11 M Na^+ 10 mM lithium cacodylate buffer.

b) Effect of pH on the denaturation curve followed at 295 nm. Circles: pH 5. Triangles: pH 5.5, squares: pH 6.0, dashed line: pH 6.5; dotted line pH 7.2; full line pH 7.8. d-TG_4T oligonucleotide at 20 μM strand concentration in a 0.11 M Na^+.

Figure S6: Effect of divalent (Mg^{2+}) cations.

a) Effects of $MgCl_2$ concentration on association rate constant k_{on} at 4°C for the d-TG_4T oligonucleotide in the presence of 0.11 M NaCl (filled circles) or 0.11 M KCl (squares).

b) Examples of melting profiles at 240 nm of the preformed $d(TG_4)_4$ quadruplex in the presence of various concentrations of $MgCl_2$ (determined at 0.18°C/min). Filled circles: no magnesium. Triangles: 3 mM; crosses: 6 mM; diamonds 10 mM, circles: 15 mM. Note that the differences in hyperchromicity are the result of incomplete quadruplex formation during the overnight incubation (higher $MgCl_2$ leads to faster association – see panel A -).

c) Effects of $MgCl_2$ concentration on $T_{1/2}$ of the $d(TG_4)_4$ quadruplex (determined at 0.18°C/min). 10 mM pH 7.2 lithium cacodylate buffer with 0.11 M NaCl.

Figure S7: k_{on} *vs.* temperature plots for 8 different sequences.

Data obtained in a 0.11 M Na^+ (filled circles) or 0.11 M K^+ (open squares) at pH 7.0 or 7.2 in a 10 mM cacodylate buffer. Sequence of the quadruplex-forming oligomer is shown on top of each panel.

References:

1. Mergny, J.L., Phan, A.T. and Lacroix, L. (1998) Following G-quartet formation by UV-spectroscopy. *FEBS Lett.*, **435,** 74-78.
2. Wallimann, P., Kennedy, R.J., Miller, J.S., Shalango, W. and Kenp, D.S. (2003) Dual Wavelength Parametric Test of Two-State Models for Circular Dichroism Spectra of Helical Polypeptides: Anomalous Dichroic Properties of Alanine-Rich Peptides. *J. Am. Chem. Soc.*, **125,** 1203-1220.
3. Uddin, M.K., Kato, Y., Takagi, Y., Mikuma, T. and Taira, K. (2004) Phosphorylation at 5' end of guanosine stretches inhibits dimerization of G-quadruplexes and formation of a G-quadruplex interferes with the enzymatic activities of DNA enzymes. *Nucleic Acids Res.*, **32,** 4618-4629.

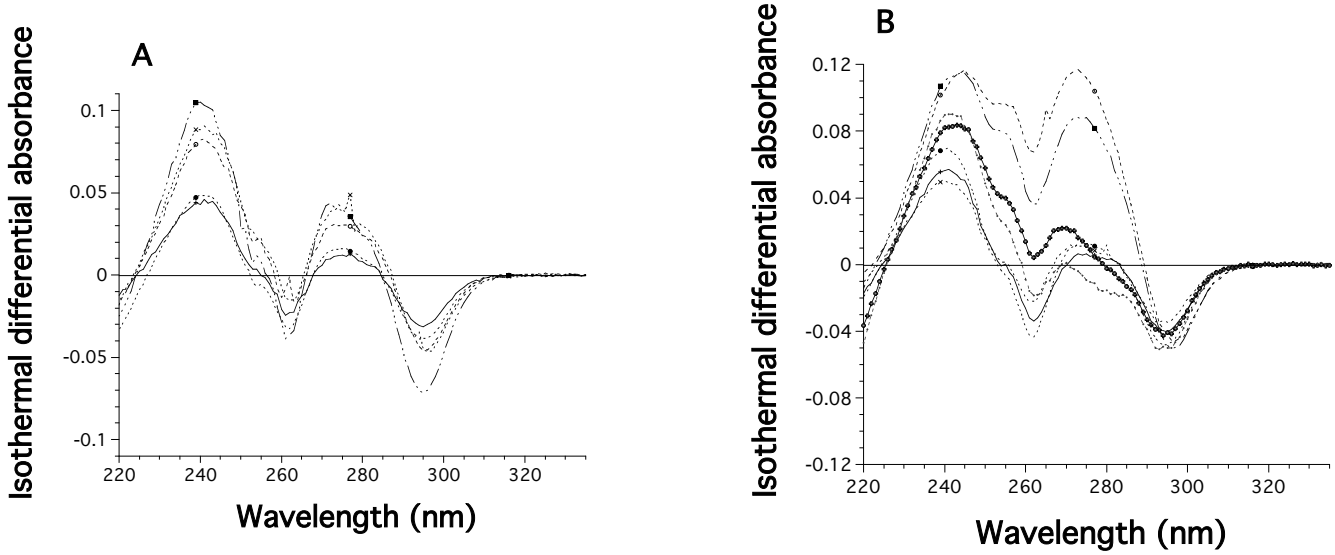
A
B
Isothermal differential absorbance
Wavelength (nm)
0.1
0.05
0
-0.05
-0.1
0.12
0.08
0.04
-0.04
-0.08
-0.12
220
240
260
280
300
320

figure S1

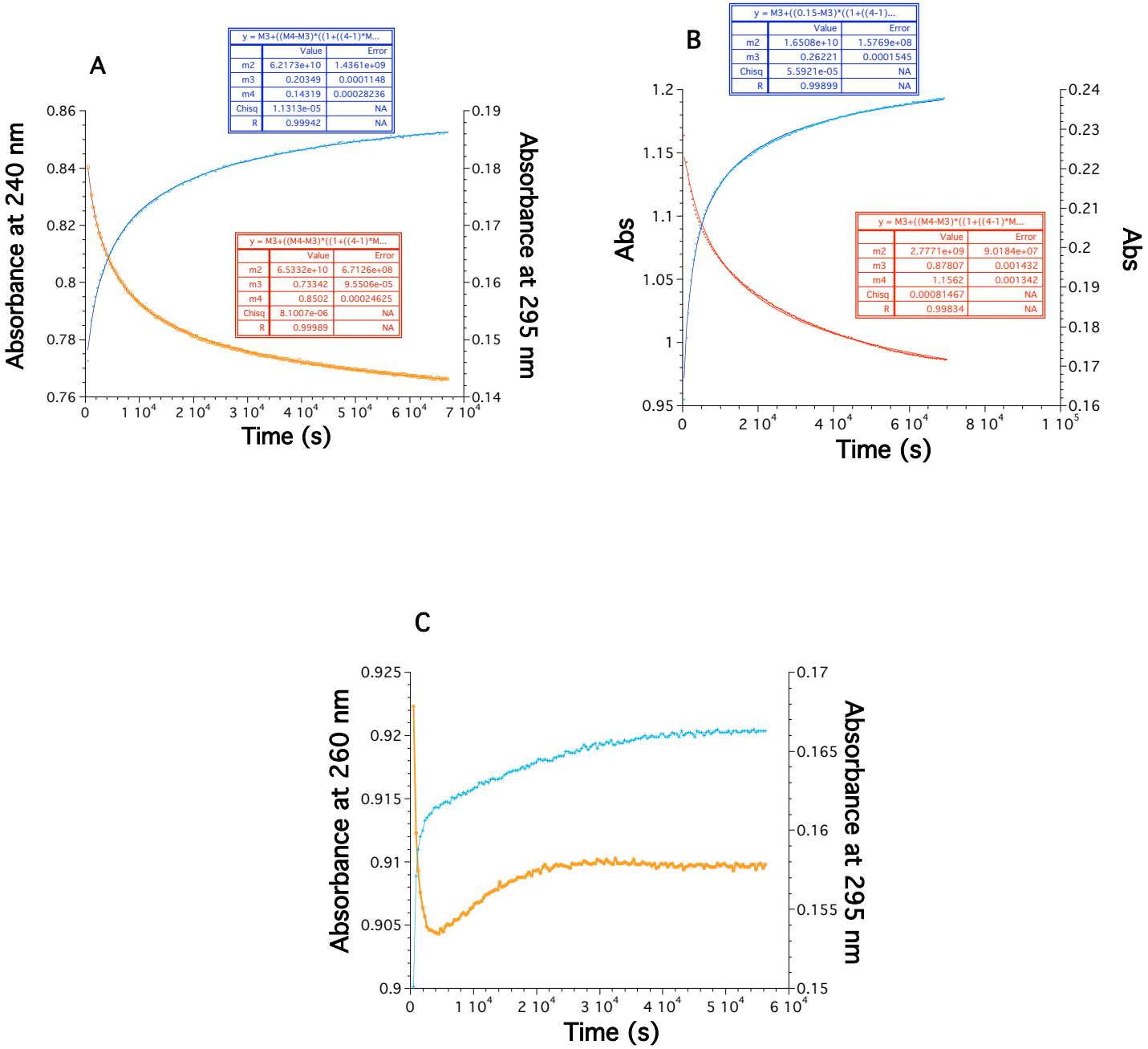
A
y = M3+((M4-M3)*((1+((4-1)*M...
Value Error
m2 6.2173e+10 1.4361e+09
m3 0.20349 0.0001148
m4 0.14319 0.00028236
Chisq 1.1313e-05 NA
R 0.99942 NA
y = M3+((M4-M3)*((1+((4-1)*M...
Value Error
m2 6.5332e+10 6.7126e+08
m3 0.73342 9.5506e-05
m4 0.8502 0.00024625
Chisq 8.1007e-06 NA
R 0.99989 NA
Absorbance at 240 nm
Absorbance at 295 nm
Time (s)
B
y = M3+((0.15-M3)*((1+((4-1)...
Value Error
m2 1.6508e+10 1.5769e+08
m3 0.26221 0.0001545
Chisq 5.5921e-05 NA
R 0.99899 NA
y = M3+((M4-M3)*((1+((4-1)*M...
Value Error
m2 2.7771e+09 9.0184e+07
m3 0.87807 0.001432
m4 1.1562 0.001342
Chisq 0.00081467 NA
R 0.99834 NA
Abs
Abs
Time (s)
C
Absorbance at 260 nm
Absorbance at 295 nm
Time (s)

figure S2

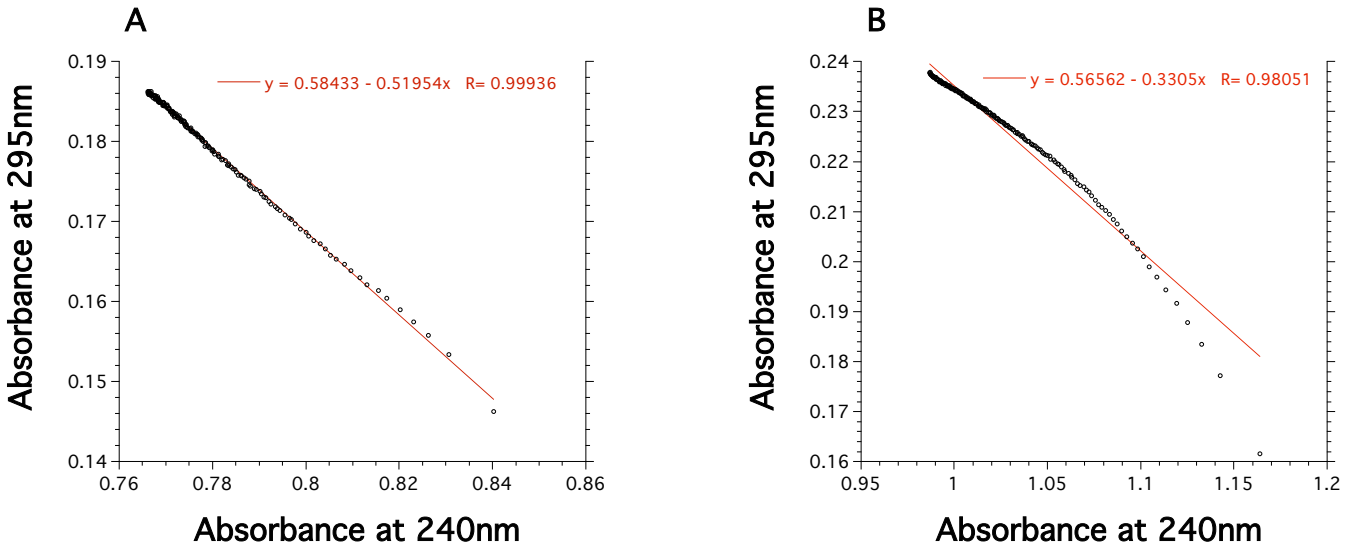
A
y = 0.58433 - 0.51954x R= 0.99936
Absorbance at 295nm
Absorbance at 240nm
0.19
0.18
0.17
0.16
0.15
0.14
0.76
0.78
0.8
0.82
0.84
0.86
B
y = 0.56562 - 0.3305x R= 0.98051
Absorbance at 295nm
Absorbance at 240nm
0.24
0.23
0.22
0.21
0.2
0.19
0.18
0.17
0.16
0.95
1
1.05
1.1
1.15
1.2

figure S3

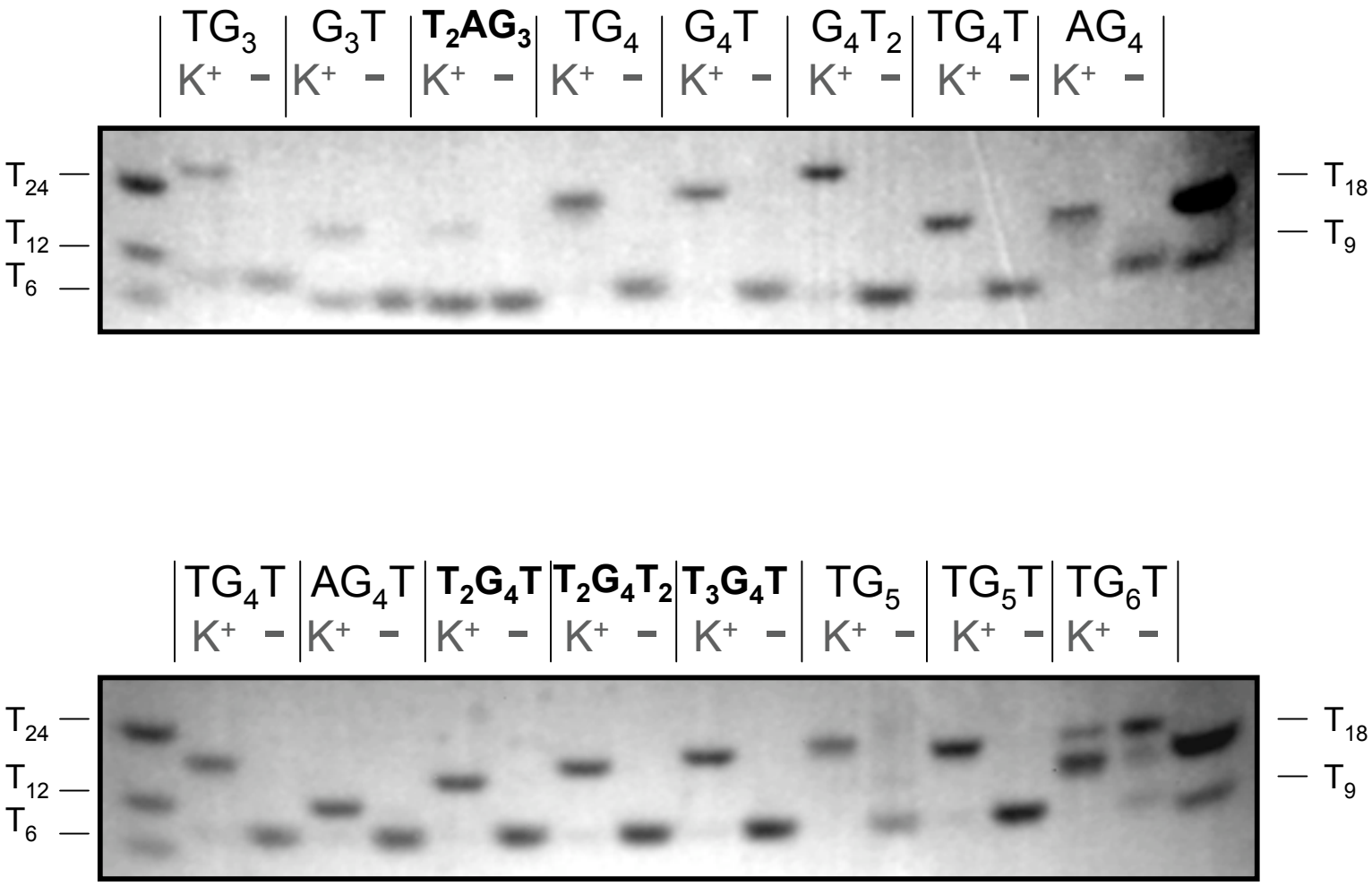
TG3
G3T
T2AG3
TG4
G4T
G4T2
TG4T
AG4
K+ -
T24
T12
T6
T18
T9
TG4T
AG4T
T2G4T
T2G4T2
T3G4T
TG5
TG5T
TG6T

figure S4

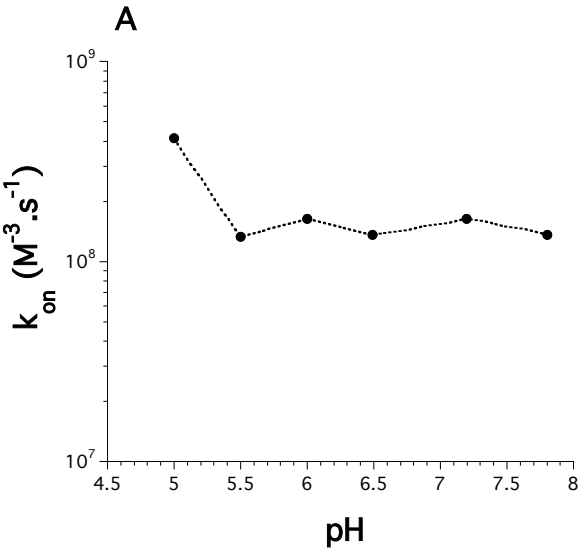
A
10^9
10^8
10^7
k_{on} ($M^{-3}.s^{-1}$)
4.5
5
5.5
6
6.5
7
7.5
8
pH

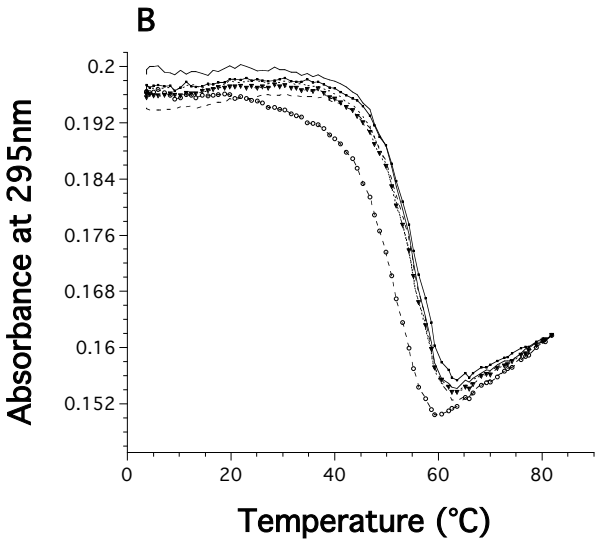
B
0.2
0.192
0.184
0.176
0.168
0.16
0.152
Absorbance at 295nm
0
20
40
60
80
Temperature (°C)

figure S5

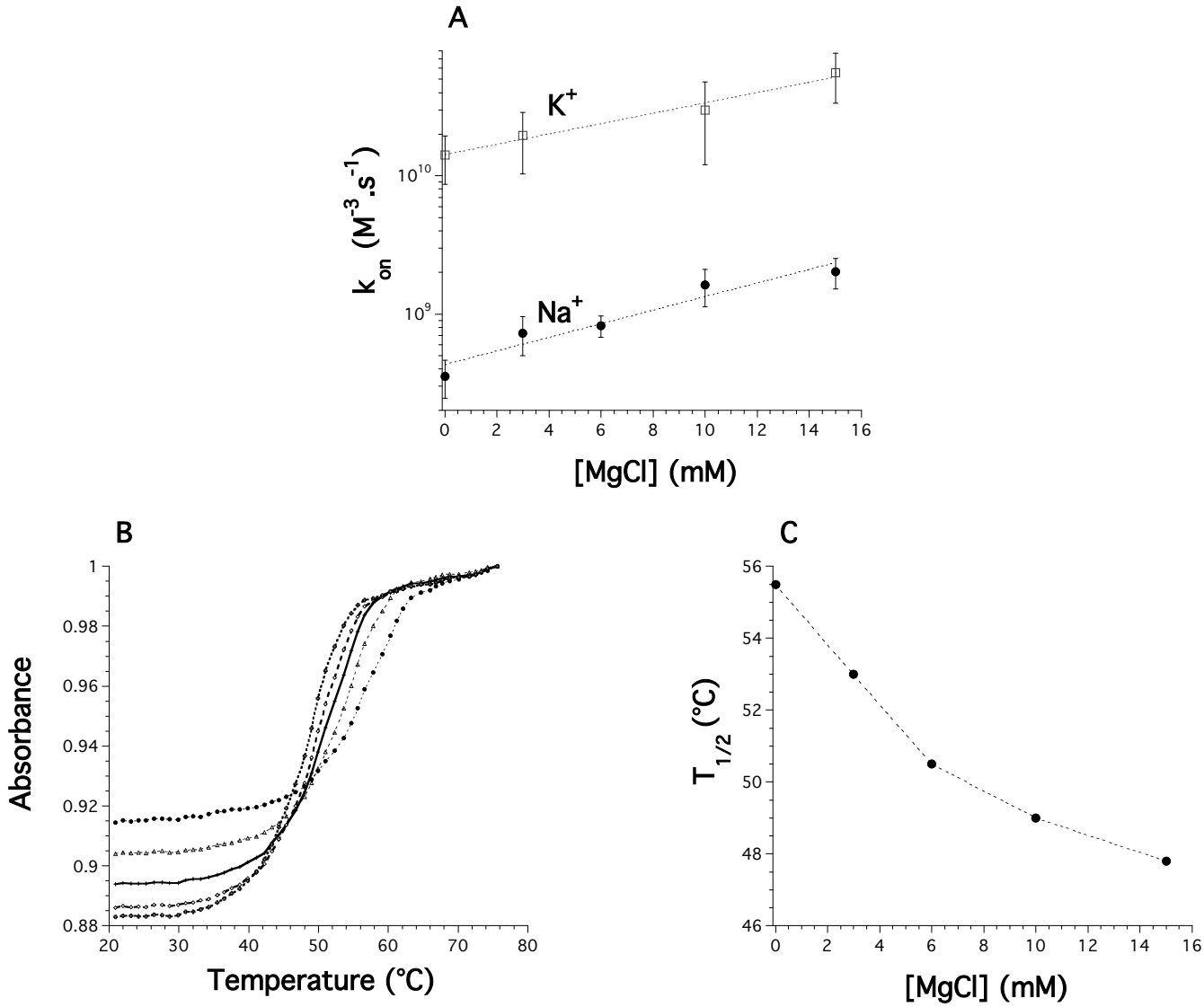
A
K+
Na+
k on (M-3.s-1)
10^10
10^9
0 2 4 6 8 10 12 14 16
[MgCl] (mM)
B
Absorbance
1 0.98 0.96 0.94 0.92 0.9 0.88
20 30 40 50 60 70 80
Temperature (°C)
C
T1/2 (°C)
56 54 52 50 48 46
0 2 4 6 8 10 12 14 16
[MgCl] (mM)

figure S6

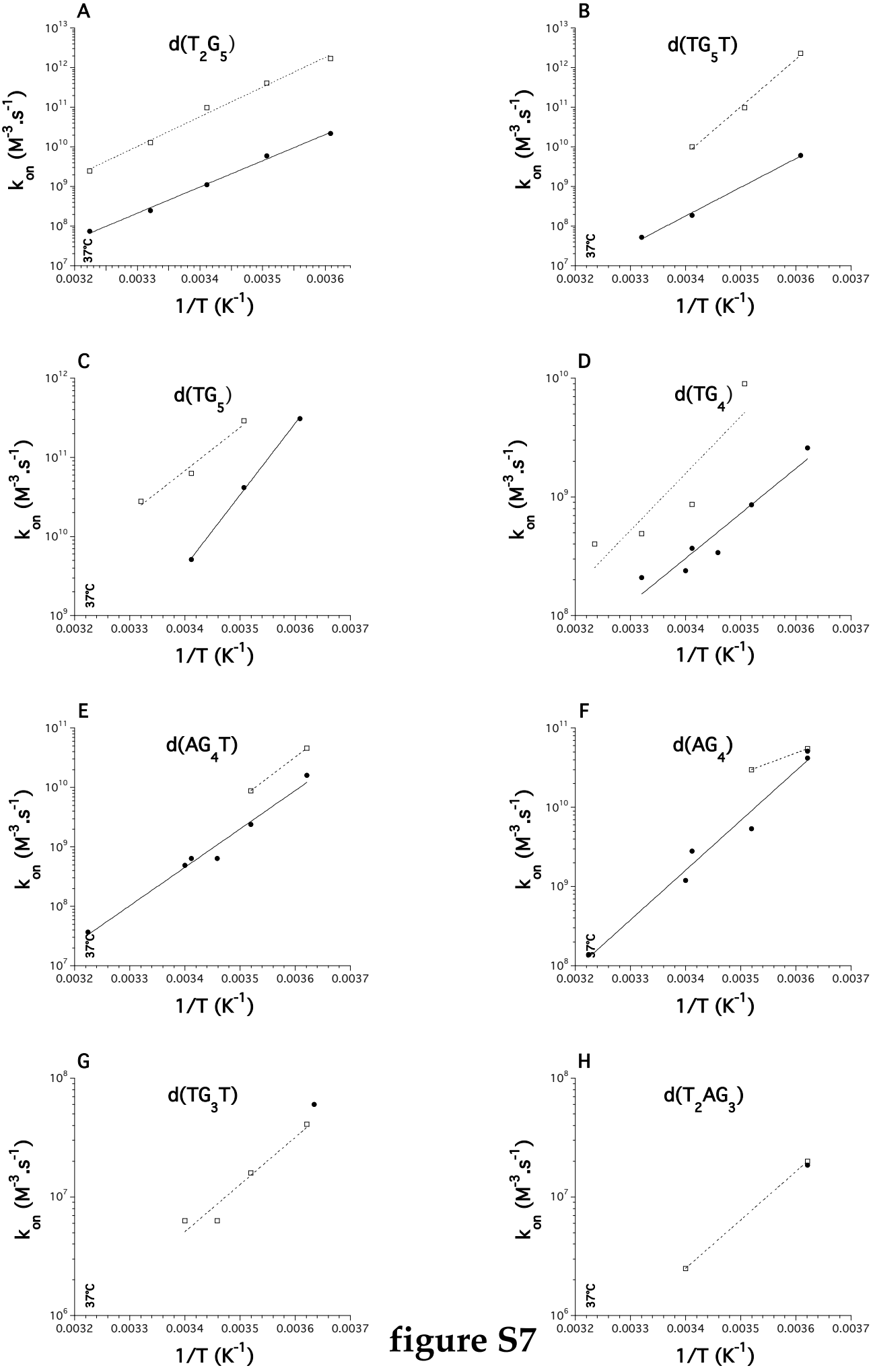
A
d(T2G5)
B
d(TG5T)
C
d(TG5)
D
d(TG4)
E
d(AG4T)
F
d(AG4)
G
d(TG3T)
H
d(T2AG3)
kon (M-3.s-1)
1/T (K-1)
37°C

figure S7